Lattice-QCD Computable Quark Correlation Functions at Three-Loop Order and Extraction of Splitting Functions

Chen Cheng,[*] Li-Hong Huang,[†] and Xiang Li[‡]
School of Physics, Peking University, Beijing 100871, China

Zheng-Yang Li[§]
Theory Center, Jefferson Lab, 12000 Jefferson Avenue, Newport News, Virginia 23606, USA

Yan-Qing Ma[‖]
School of Physics, Peking University, Beijing 100871, China
and Center for High Energy Physics, Peking University, Beijing 100871, China

(Received 6 November 2024; revised 16 May 2025; accepted 30 May 2025; published 24 June 2025)

We present the first complete next-to-next-to-next-to-leading-order calculation of the matching coefficients that link unpolarized flavor nonsinglet parton distribution functions with lattice QCD computable correlation functions. By using this high-order result, we notice a reduction in theoretical uncertainties compared to relying solely on previously known lower-order matching coefficients. Furthermore, based on this result we have extracted the three-loop unpolarized flavor nonsinglet splitting function, which is in agreement with the state-of-the-art result. Because of the simplicity of our method, it has the potential to advance the calculation of splitting functions to the desired four-loop order.

DOI: 10.1103/53ys-3n19

Introduction—Parton distribution functions (PDFs) are important nonperturbative quantities that describe the one-dimensional internal structure of colliding hadrons. Since PDFs obey the Dokshitzer-Gribov-Lipatov-Altarelli-Parisi evolution equations [1–3], whose kernel known as the splitting function can be computed perturbatively, it is sufficient to determine the PDFs at a specific renormalization scale. Presently, PDFs have been extracted from high-precision collider data [4–11]. To further enhance the accuracy of PDFs, it is crucial to compute the splitting functions to next-to-next-to-next-to-leading order (N3LO), i.e., four-loop order. Nevertheless, due to their complexity, the N3LO results are only known approximately so far [12–19].

In addition to being extracted from experimental data, the first-principles lattice QCD (LQCD) calculations of PDFs are also extremely significant. Over the past decade, stimulated by the large momentum effective field theory [20,21], new approaches for investigating PDFs through LQCD calculations have been developed and have led to tremendous breakthroughs in this field [22]. The new methods include quantities such as quasi-PDFs [20], pseudo-PDFs [23], current-current correlators in momentum space [24], and current-current correlators in position space [25]. These quantities can also be interpreted as good lattice cross sections [25,26], which are calculable using LQCD and factorizable to the universal PDFs, allowing us to extract PDFs from LQCD computations. Therefore, when using these methods, in addition to LQCD computations, it is crucial to compute the matching coefficients of factorization relations in perturbative QCD.

For the extraction of unpolarized flavor nonsinglet PDFs, perturbative calculations have been carried out up to the next-to-next-to-leading order (NNLO) [27,28]. Based on these calculations, the unpolarized valence PDFs of both the pion and the proton have been obtained at the NNLO level through the analysis of LQCD computations [29–33]. These studies suggest that, for the extraction of PDFs, the NNLO corrections are generally smaller than the next-to-leading-order (NLO) corrections, indicating good perturbative convergence, which is crucial for precise calculations. Moreover, it was found that the NNLO results can lead to a reduction in scale-variation uncertainties compared to relying solely on NLO results. The aforementioned characteristics, along with the necessity of achieving high-precision PDFs, highlight the significance of higher-order perturbative calculations.

[*]Contact author: 1801214966@pku.edu.cn
[†]Contact author: lhhuang@pku.edu.cn
[‡]Contact author: lix-PHY@pku.edu.cn
[§]Contact author: zyli@jlab.org
[‖]Contact author: yqma@pku.edu.cn

Published by the American Physical Society under the terms of the Creative Commons Attribution 4.0 International license. Further distribution of this work must maintain attribution to the author(s) and the published article's title, journal citation, and DOI. Funded by SCOAP[3].

In this Letter, we derive for the first time the N3LO nonsinglet matching coefficients of the quark correlation function. By applying the N3LO matching coefficients to the valence-quark correlation functions, we show an improvement in perturbative uncertainty. Furthermore, based on the obtained divergent part of the quark correlation function, we successfully extract the three-loop (or NNLO) unpolarized flavor nonsinglet splitting function, which is in agreement with that obtained in the literature. Our method is much simpler than traditional method using deep-inelastic structure functions [34], and it may provide a feasible way to advance the calculation of the splitting functions to the desired N3LO.

Quark correlation functions—Our Letter centers on the unpolarized gauge invariant quark correlation operator

$$\mathcal{O}_q^{\nu,b}(\xi,\mu^2;\delta)=\bar{\psi}_q^b(\xi)\gamma^\nu\Phi^{(f)}(\xi,0)\psi_q^b(0)|_{\mu^2,\delta}, \quad (1)$$

which has been utilized to define quasi-PDFs in Ref. [20]. The operator is composed of bare fields with a path-ordered gauge link in fundamental representation, $\Phi^{(f)}(\xi,0)=\mathcal{P}e^{-ig_s\int_0^1 dr\xi\cdot\mathbf{A}^{(f)}(r\xi)}$, where ξ is a spacelike interval satisfying $\xi_0=0$ and $\mathbf{A}^{(f)}\equiv T^a\mathbf{A}^a$ is the Lie-algebra-valued gauge field in fundamental representation. In the above definition, δ is the ultraviolet (UV) regulator and μ is the UV renormalization scale. The UV divergences of the operator are known to be multiplicatively renormalizable [35–37] as

$$\mathcal{O}_q^{\nu,\mathrm{RS}}(\xi,\mu^2)=\mathcal{O}_q^{\nu,b}(\xi,\mu^2;\delta)/Z^{\mathrm{RS}}(\xi^2,\mu^2;\delta), \quad (2)$$

where the superscript RS indicates a renormalization scheme and the renormalized operator is insensitive to the regulator δ.

Quark correlation functions (QCFs) are defined as the hadronic matrix elements of $\mathcal{O}_q^{\nu,\mathrm{RS}}$,

$$F_{q/h}^{\nu,\mathrm{RS}}(\omega,\xi^2,\mu^2)=\langle h(p)|\mathcal{O}_q^{\nu,\mathrm{RS}}(\xi,\mu^2)|h(p)\rangle, \quad (3)$$

where $|h(p)\rangle$ is the state of a hadron h with momentum p and $\omega\equiv p\cdot\xi$. With $\xi^2\Lambda_{\mathrm{QCD}}^2\ll 1$, $F_{q/h}^{\nu,\mathrm{RS}}$ are calculable on LQCD and factorizable into PDFs [25,26,38]. Without loss of generality, we will assume that ξ has only z component in the rest of the Letter but that the Lorentz index ν can be chosen freely as either the time component or a space component. In this Letter, we focus on flavor nonsinglet QCFs defined as

$$F_{q_{ik}/h}^{\nu,\mathrm{RS}}(\omega,\xi^2,\mu^2)\equiv F_{q_i/h}^{\nu,\mathrm{RS}}(\omega,\xi^2,\mu^2)-F_{q_k/h}^{\nu,\mathrm{RS}}(\omega,\xi^2,\mu^2). \quad (4)$$

As any renormalization scheme RS can be related to the modified minimal subtraction ($\overline{\mathrm{MS}}$) scheme as

$$F_{q_{ik}/h}^{\nu,\mathrm{RS}}(\omega,\xi^2,\mu^2)=F_{q_{ik}/h}^{\nu,\overline{\mathrm{MS}}}(\omega,\xi^2,\mu^2)/R^{\mathrm{RS}}(\xi^2,\mu^2), \quad (5)$$

where $R^{\mathrm{RS}}(\xi^2,\mu^2)=Z^{\mathrm{RS}}(\xi^2,\mu^2;\delta)/Z^{\overline{\mathrm{MS}}}(\xi^2,\mu^2;\delta)$ is the finite renormalization factor. We will only focus on the $\overline{\mathrm{MS}}$ renormalization scheme.

The flavor nonsinglet QCFs in the $\overline{\mathrm{MS}}$ scheme possess the following collinear factorization formula:

$$F_{q_{ik}/h}^{\nu,\overline{\mathrm{MS}}}(\omega,\xi^2,\mu^2)=\int_{-1}^1\frac{\mathrm{d}x}{x}f_{q_{ik}/h}(x,\mu^2)K^\nu(x\omega,\xi^2,\mu^2), \quad (6)$$

with corrections at $O(\xi^2\Lambda_{\mathrm{QCD}}^2)$, where we have not differentiated the renormalization scale from the factorization scale. $f_{q_{ik}/h}(x,\mu^2)\equiv f_{q_i/h}(x,\mu^2)-f_{q_k/h}(x,\mu^2)$ is the flavor nonsinglet PDF renormalized in $\overline{\mathrm{MS}}$ scheme, and K^ν are perturbative matching coefficients, which will be computed to N3LO in this Letter.

As $Z^{\overline{\mathrm{MS}}}(\xi^2,\mu^2;\delta)$ is the renormalization factor of the quark correlation operator and is independent of the property of the hadron h and its momentum, it can be obtained by

$$Z^{\overline{\mathrm{MS}}}(\xi^2,\mu^2;\delta)=\left.\frac{\tilde{p}_\nu F_{q_{ik}/q_i}^{\nu,b}(\omega,\xi^2,\mu^2;\delta)}{\tilde{p}_\nu F_{q_{ik}/q_i}^{\nu,\overline{\mathrm{MS}}}(\omega,\xi^2,\mu^2)}\right|_{\omega\to 0}, \quad (7)$$

where we replace the hadron h by a parton q_i and define

$$\tilde{p}_\nu=\xi_\nu/\omega-\xi^2p_\nu/\omega^2, \quad (8)$$

which effectively projects out the time component.

Result of matching coefficients—As K^ν are independent of the hadronic state $|h\rangle$, we replace the hadronic state in Eq. (6) by a quark state and expand the formula perturbatively as

$$F_{q_{ik}/q_i}^{\nu,(n)}(\omega,\xi^2,\mu^2,\epsilon)=\sum_{m=0}^n\int_{-1}^1\frac{dx}{x}f_{q_{ik}/q_i}^{(m)}(x,\mu^2,\epsilon)K^{\nu,(n-m)}(x\omega,\xi^2,\mu^2,\epsilon), \quad (9)$$

with $n,m=0,1,2,3$ indicating the power of α_s and $f_{q_{ik}/q_i}^{(n)}$ being a partonic PDF in the $\overline{\mathrm{MS}}$ scheme [34,39]. Note that, for partonic quantities, we use dimensional regularization with $D=4-2\epsilon$ to regularize both UV divergences and infrared and collinear divergences. Once $f_{q_{ik}/q_i}^{(n)}$ are known, we can derive the N3LO matching coefficient $K^{\nu(n)}$ by calculating $F_{q_{ik}/q_i}^{\nu,(n)}$ up to $n=3$.

In Fig. 1, we show some representative Feynman diagrams for $F_{q_{ik}/q_i}^{\nu,(n)}$. With $f_{q_{ik}/q_i}^{(0)}(x)=\delta(1-x)$, the diagram (a) gives the tree level result

$$K^{\nu,(0)}(\omega)=F_{q_{ik}/q_i}^{\nu,(0)}(\omega)=-2\mathrm{i}p^\nu e^{\mathrm{i}\omega}. \quad (10)$$

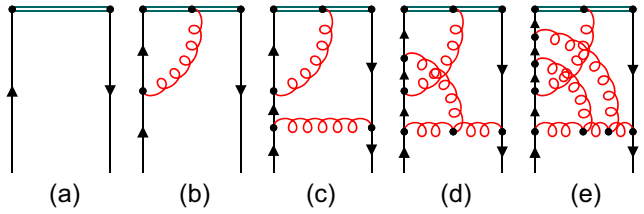

FIG. 1. Representative Feynman diagrams for QCFs at LO (a), NLO (b), NNLO (c), N3LO (d), and next-to-next-to-next-to-next-to-leading-order (N4LO) (e). The double line represents the gauge link.

For diagrams at high orders, the amplitudes contain loop integrals and path-ordered integrals along the gauge link. For example, three-loop diagram (d) gives the integral

$$I_{\vec{\nu}}(\omega,\xi^2;\epsilon)=\int_0^1 \mathrm{d}r\int\prod_{i=1}^{3}\frac{\mathrm{d}^D l_i}{(2\pi)^D}\frac{\text{numerator}}{\mathcal{D}_1^{\nu_1}\cdots\mathcal{D}_8^{\nu_8}}e^{\mathrm{i}(rl_2+l_3)\cdot\xi}, \tag{11}$$

where the propagators are defined as

$$\begin{aligned}&\mathcal{D}_1={l_1}^2,\mathcal{D}_2={l_2}^2,\mathcal{D}_3={l_3}^2,\mathcal{D}_4=(l_1+l_3)^2,\\&\mathcal{D}_5=(l_2+l_3)^2,\mathcal{D}_6=(l_1-p)^2,\mathcal{D}_7=(l_3-p)^2,\\&\mathcal{D}_8=(l_1+l_2+l_3)^2.\end{aligned} \tag{12}$$

As explained in Ref. [28], the exponential parts can be transformed to linear propagators in momentum space by using

$$\begin{aligned}&\int d\xi_z e^{-\mathrm{i}q_z\xi_z}\xi_z^{\delta_j}\int_0^1 dr e^{-\mathrm{i}(rl_{2z}+l_{3z})\xi_z}\\&\quad=2\mathrm{i}\,\mathrm{Im}\frac{1}{(l_{2z}+l_{3z}+\tilde{q}_z)(l_{3z}+\tilde{q}_z)},\end{aligned} \tag{13}$$

where $\tilde{q}_z=q_z+\mathrm{i}0^+$ and $2\pi\delta(x)=-2\,\mathrm{Im}(1/x+\mathrm{i}0^+)$ has been used.

After performing the aforementioned transformation, loop integrals in momentum space are suitable to be handled using integration-by-parts (IBP) relations [40,41] to express them as linear combinations of a small set of integrals, called master integrals (MIs). We use the package BLADE [42,43] for reduction, which accelerates the IBP reduction by using block-triangular form [43], and use LITERED+FINITEFLOW [44,45] to perform a cross-check. For the integrals defined in Eq. (11), there are 97 MIs, which have been selected solely through the Laporta algorithm, without any additional modifications or adjustments.

Any MI generated from $F^{\nu,(n)}_{q_{ik}/q_i}$ can be expressed as

$$I_j(p_z,q_z;\epsilon)=|q_z|^{(-1-2n\epsilon)}q_z^{\delta_j}J_j(y;\epsilon), \tag{14}$$

where $y=p_z/q_z$ and $\delta_j-1-2n\epsilon$ is the mass dimension of I_j. By applying IBP reduction, the differential equations of $J_j(y;\epsilon)$ can be constructed as [46]

$$\frac{\partial}{\partial y}\vec{J}(y;\epsilon)=A(y;\epsilon)\vec{J}(y;\epsilon). \tag{15}$$

The boundary conditions $J_j(0;\epsilon)$ are vacuum integrals with linear propagators at n-loop order, which can be calculated by the method of auxiliary mass flow [47–52]. Based on the differential equations and boundary conditions, $J_j(y;\epsilon)$ can be expanded as a Taylor series of y to any needed order. Therefore, we can obtain results of QCFs as a Taylor series of y by combining the coefficients of reduction and MIs. We then transform the results to position space by inverse Fourier transformation, and the series of y will be transformed to series of ω.

By adding contributions from all diagrams, applying the UV renormalization factor in the $\overline{\mathrm{MS}}$ scheme and using the factorization formula (9), we obtain the matching coefficients $K^{\nu(n)}$ up to N3LO. All divergences are canceled and the results of $K^{\nu(n)}$ are finite after taking $\epsilon\to 0$, which verifies the proof of the factorization theorem [26]. We have also checked that the running of $K^{\nu(n)}$ with scale μ for each order of ω agrees with the renormalization group equation constructed by $\mathrm{d}F^{\nu,b}/\mathrm{d}\ln\mu^2=0$. Our NLO and NNLO results agree with previous calculations in Ref. [25,28], and the terms proportional to $C_F N_f^2$ in the N3LO results agree with calculations using another method from Ref. [53]. The new results at N3LO are given analytically up to $O(\omega^5)$ and numerically up to $O(\omega^{100})$ in Supplemental Material (SM) [54]. Regarding the analytical outcomes, apart from ω, the color factors, the number of flavors n_f, and the term $\ln(-\xi^2\mu^2/4)+2\gamma_E$, the only nonrational numbers we come across are the Riemann zeta functions $\zeta(n)$ where n takes on the values of 2, 3, 4, and 5. Given that the ω expansion of K has an infinite convergent radius [25], these results can be used to compute the matching coefficients $K^{\nu(3)}$ up to $|\omega|=20$ with at least nine significant digits, and up to $|\omega|=35$ with at least three significant digits, much more than sufficient for the requirement of lattice computations [29–33].

By choosing q_k as $\bar{q}_i$, we obtain valence-quark correlation functions. In this case, the factorization formula in Eq. (6) is modified as

$$F^{\nu,\overline{\mathrm{MS}}}_{q_v/h}(\omega,\xi^2,\mu^2)=\int_0^1\frac{dx}{x}f_{q_v/h}(x,\mu^2)K^{\nu}_v(x\omega,\xi^2,\mu^2), \tag{16}$$

where $q_v\equiv q_i-\bar{q}_i$, $F^{\nu,\overline{\mathrm{MS}}}_{q_v/h}(\omega,\xi^2,\mu^2)\equiv F^{\nu,\overline{\mathrm{MS}}}_{q_i/h}(\omega,\xi^2,\mu^2)-F^{\nu,\overline{\mathrm{MS}}}_{\bar{q}_i/h}(\omega,\xi^2,\mu^2)$, $f_{q_v/h}(x,\mu^2)\equiv f_{q_i/h}(x,\mu^2)-f_{\bar{q}_i/h}(x,\mu^2)$ and $K^{\nu}_v(x\omega,\xi^2,\mu^2)\equiv K^{\nu}(x\omega,\xi^2,\mu^2)-K^{\nu}(-x\omega,\xi^2,\mu^2)$. With the obtained three-loop results of K^{ν}, we can predict

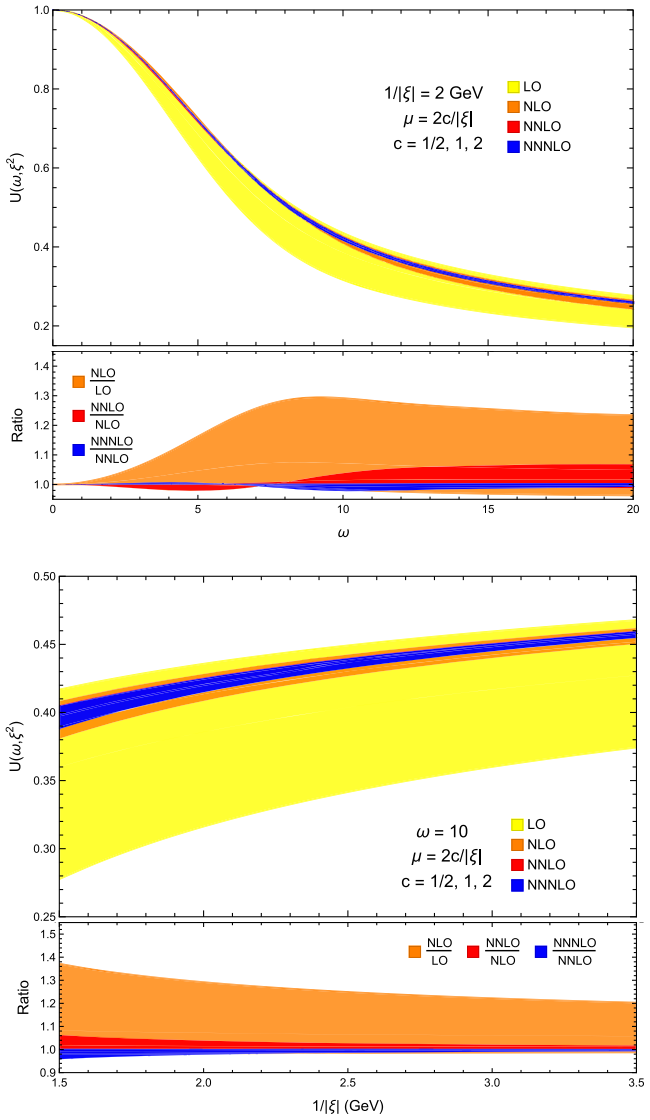

FIG. 2. Numerical predictions for valence-quark correlation functions defined in Eq. (17) with LO, NLO, NNLO and NNNLO matching coefficients and CT18NNLO PDFs.

valence-quark correlation functions by using existing PDFs extracted from experimental data. In Fig. 2, we present

$$U(\omega,\xi^2) \equiv \frac{\tilde{p}\cdot F_{q_v/h}(\omega,\xi^2)}{\lim_{\omega\to 0}\tilde{p}\cdot F_{q_v/h}(\omega,\xi^2)} \tag{17}$$

either as a function of ω with a fixed $1/|\xi| = 2$ GeV, or as a function of $1/|\xi|$ with a fixed $\omega = 10$. As the N3LO PDF is not available, we use CT18NNLO PDFs [6] as our input, and set $\mu = 2c/|\xi|$ to minimize logarithms encountered in perturbative calculation. We vary $c = \frac{1}{2}, 1, 2$ for the bands to estimate theoretical uncertainties due to the ambiguity of scale choice. Our results show an improvement in perturbative uncertainty when N3LO matching coefficients are used.

Owing to the limitations of computational power, the value of $1/|\xi|$ for lattice data cannot be excessively large, as evidenced in the Refs. [29–33]. In order to more effectively constrain the PDFs, one is often compelled to utilize lattice data with a smaller value of $1/|\xi|$. Under such circumstances, higher-order corrections are even more crucial and our N3LO results play an indispensable role in establishing a reliable connection between the lattice data and the PDFs.

Extraction of splitting functions—In the $\overline{\text{MS}}$ renormalization scheme, flavor nonsinglet PDFs satisfy a diagonalized Dokshitzer-Gribov-Lipatov-Altarelli-Parisi equation [1–3],

$$\frac{d}{d\ln\mu^2} f^{\pm}_{ns}(x,\mu^2,\epsilon) = \int_x^1 \frac{dz}{z} P^{\pm}_{ns}\left(\frac{x}{z},\mu^2\right) f^{\pm}_{ns}(z,\mu^2,\epsilon), \tag{18}$$

where $f^{\pm}_{ns}(x) = f_{q_{ik}/q_i}(x) \pm f_{\bar{q}_{ik}/q_i}(x)$ and $P^{\pm}_{ns}$ are splitting functions. Partonic level nonsinglet PDFs and splitting functions can be perturbatively expanded as

$$f^{\pm}_{ns}(x,\mu^2,\epsilon) = \delta(1-x) + \sum_{n=1}^{\infty}\sum_{i=1}^{n} \alpha_s^n \frac{f^{\pm(n,i)}_{ns}(x)}{\epsilon^i}, \tag{19}$$

$$P^{\pm}_{ns}(x,\mu^2) = \sum_{n=1}^{\infty} \alpha_s^n P^{\pm(n)}_{ns}(x), \tag{20}$$

and our goal is to extract $P^{\pm(3)}_{ns}$.

By inserting Eqs. (20) and (19) into Eq. (18) and using the running coupling equations of α_s [55], we obtain the solution as

$$f^{\pm(n,1)}_{ns}(x) = -\frac{P^{\pm(n)}_{ns}(x)}{n}, \tag{21}$$

which expresses the ϵ^{-1} pole of the n-loop partonic PDF by the n-loop splitting function.

We assume that $f^{\pm(j,i)}_{ns}$ and $K^{\nu(j)}$ are known for $j < n$ and rearrange Eq. (9) by moving known results to the left-hand side of the equation to obtain

$$\tilde{F}^{\nu,(n)}_{q_{ik}/q_i}(\omega,\xi^2,\mu^2,\epsilon) = \text{finite terms} + \frac{1}{\epsilon}\int_{-1}^{1}\frac{dx}{x} f^{(n,1)}_{q_{ik}/q_i}(x) \times K^{\nu(0)}(x\omega,\xi^2,\mu^2,\epsilon), \tag{22}$$

where $\tilde{F}^{\nu,(n)}_{q_{ik}/q_i}$ represents new left-hand side after rearranging. Making use of the relation $f_{q_i/h}(x) = -f_{\bar{q}_i/h}(-x)$ and Eq. (10), we obtain the ϵ^{-1} pole of Eq. (22) as the following form:

$$
\begin{aligned}
&-2\mathrm{i}\int_{-1}^{1}\frac{\mathrm{d}x}{x}f^{(n,1)}_{q_{ik}/q_i}(x)\times xp^{\nu}e^{\mathrm{i}x\omega}\\
&=\frac{2\mathrm{i}}{n}\int_0^1 \mathrm{d}x[\cos(x\omega)P^{-(n)}_{ns}(x)+\mathrm{i}\sin(x\omega)P^{+(n)}_{ns}(x)]\\
&=\frac{2\mathrm{i}}{n}\left[\sum_{N=0}^{\infty}\frac{(-1)^N}{(2N)!}\gamma^{-(n)}_{ns}(2N+1)\omega^{2N}\right.\\
&\quad\left.+\sum_{N=0}^{\infty}\mathrm{i}\frac{(-1)^N}{(2N+1)!}\gamma^{+(n)}_{ns}(2N+2)\omega^{2N+1}\right],
\end{aligned}
\tag{23}
$$

where $\gamma^{\pm(n)}_{ns}(N)$ is the Mellin transformation of $P^{\pm(n)}_{ns}(x)$. Therefore, with the series expansion of ω for the divergent part of $F^{\nu,(n)}_{q_{ik}/q_i}$, we can extract $\gamma^{\pm(n)}_{ns}(N)$ from each order of ω and eventually obtain $P^{\pm(n)}_{ns}(x)$ by inverse Mellin transformation. By computing ω series to 1000 orders, we have successfully extracted $P^{(3)}_{ns}(x)$, which agrees with the state-of-the-art result in Ref. [34].

Compared with the traditional approach of extracting splitting functions through the utilization of deep-inelastic structure functions [34], our methodology employing QCFs offers substantial advantages. One key benefit is the notable reduction in the number of Feynman diagrams, a distinction that is already evident at the tree level order. At this order, our method has only one Feynman diagram, as illustrated in Fig. 1(a). In contrast, the approach based on deep-inelastic structure functions requires two Feynman diagrams. More crucially, as we will elaborate in the subsequent discussion, the existence of the gauge link allows us to devise a strategy that significantly streamlines the process of Feynman integrals reduction, which is the primary bottleneck in the computation of four-loop splitting functions using traditional methods.

To illustrate this point, let us consider the three-loop integral in Eq. (11) as an example. By introducing the identity $1=\int \mathrm{d}^D q\delta^{(D)}(rl_2+l_3-q)$, the integration is transformed into

$$
\int_0^1 \mathrm{d}r\int\frac{\mathrm{d}^D q}{(2\pi)^D}e^{\mathrm{i}q\cdot\xi}\int\prod_{i=1}^{2}\frac{\mathrm{d}^D l_i}{(2\pi)^D}\frac{\text{numerator}}{\mathcal{D}_1^{\nu_1}\cdots\mathcal{D}_8^{\nu_8}},
\tag{24}
$$

where within the integrand, we have replaced l_3 by $q-rl_2$. Prior to integrating over r and q, the remaining portion of the expression features the same number of external vectors (p and q as compared to p and ξ in the original form) but one fewer loop momenta when contrasted with Eq. (11). This makes the computation of this part considerably simpler. After integrating out the loop momenta l_1 and l_2, by representing the resulting expression as linear combination of two-loop MIs, we can carry out a straightforward Taylor expansion of $p\cdot q/q^2$. Subsequently, the integration over q can be solved analytically. Finally, the integration over r can be accomplished through IBP reduction of r. The final result is expressed as a series of ω. This strategy is applicable for any Feynman diagram at any loop order, effectively reducing the number of loops by one. It is important to note that this strategy is feasible due to the presence of the gauge link, which leads to a linear combination of loop momenta in an exponential form within the coordinate space.

As a benchmark for evaluating the efficiency of our method, when using 32 CPU cores, the reduction of Feynman integrals for the diagram in Fig. 1(d) takes 4408 s using our original method. In contrast, when our new strategy is employed, the time required is significantly reduced to 173 s. For comparison, when dealing with a similar diagram in the context of deep-inelastic scattering structure functions, where the gauge link is replaced by a quark line, the process takes 5426 s. Taking into account the fact that our QCF-based method involves fewer Feynman diagrams, the time consumption of our approach is reduced by a factor of more than 30 compared to the traditional method based on structure functions at this order.

Moreover, we have conducted a preliminary test on a four-loop diagram, specifically Fig. 1(e). Our novel strategy has demonstrated the ability to reduce the computational time from 42 h to just 0.5 h when utilizing 32 CPU cores. This result instills optimism regarding the feasibility of extracting four-loop splitting functions using QCFs.

Summary—Quark correlation functions (QCFs) are calculable in LQCD and factorizable to PDFs [25,26,38], thus establishing connections between perturbative QCD and LQCD. For the first time, we calculate the complete N3LO unpolarized flavor nonsinglet matching coefficients for QCFs in the $\overline{\mathrm{MS}}$ renormalization scheme. With these N3LO coefficient functions and existing PDFs, we predict the valence-quark correlation function as shown in Fig. 2. This indicates a reduction in scale-variation uncertainties compared to NNLO results, demonstrating convergence as higher-order corrections are considered. Comparing our predictions with future LQCD results will enable the extraction of N3LO PDFs.

Furthermore, based on the divergent part of QCFs, we have successfully derived the flavor nonsinglet splitting function up to the three-loop level, which is consistent with the results in the literature. The inherent simplicity of QCFs offers a significant advantage, enabling us to reduce the computational time required for extracting the splitting functions by 2 orders of magnitude at four-loop level. This remarkable improvement in efficiency makes us highly optimistic about the feasibility of obtaining the four-loop splitting functions, which are of utmost importance in the current research context.

Feynman diagrams are drawn using the FEYNGAME program [56].

Acknowledgments—We thank X. Guan and Z. Liu for many helpful discussions. The work was supported in part

by the National Natural Science Foundation of China (Grants No. 12325503, No. 11975029), the National Key Research and Development Program of China under Contract No. 2020YFA0406400. Z. L. was supported in part by the U.S. Department of Energy (DOE) Contract No. DE-AC05-06OR23177. We acknowledge the computational support from the High-Performance Computing Platform of Peking University.

[1] V. N. Gribov and L. N. Lipatov, Deep inelastic e p scattering in perturbation theory, Sov. J. Nucl. Phys. **15**, 438 (1972).
[2] G. Altarelli and G. Parisi, Asymptotic freedom in Parton language, Nucl. Phys. **B126**, 298 (1977).
[3] Y. L. Dokshitzer, Calculation of the structure functions for deep inelastic scattering and e^+e^- annihilation by perturbation theory in quantum chromodynamics, Sov. Phys. JETP **46**, 64 (1977).
[4] A. Accardi, L. T. Brady, W. Melnitchouk, J. F. Owens, and N. Sato, Constraints on large-x parton distributions from new weak boson production and deep-inelastic scattering data, Phys. Rev. D **93**, 114017 (2016).
[5] S. Alekhin, J. Blümlein, S. Moch, and R. Placakyte, Parton distribution functions, α_s, and heavy-quark masses for LHC Run II, Phys. Rev. D **96**, 014011 (2017).
[6] T.-J. Hou *et al.*, New CTEQ global analysis of quantum chromodynamics with high-precision data from the LHC, Phys. Rev. D **103**, 014013 (2021).
[7] S. Bailey, T. Cridge, L. A. Harland-Lang, A. D. Martin, and R. S. Thorne, Parton distributions from LHC, HERA, tevatron and fixed target data: MSHT20 PDFs, Eur. Phys. J. C **81**, 341 (2021).
[8] R. D. Ball *et al.* (NNPDF Collaboration), Parton distributions from high-precision collider data, Eur. Phys. J. C **77**, 663 (2017).
[9] R. D. Ball *et al.* (NNPDF Collaboration), The path to proton structure at 1% accuracy, Eur. Phys. J. C **82**, 428 (2022).
[10] G. Aad *et al.* (ATLAS Collaboration), Determination of the parton distribution functions of the proton using diverse ATLAS data from pp collisions at $\sqrt{s} = 7$, 8 and 13 TeV, Eur. Phys. J. C **82**, 438 (2022).
[11] I. Sitiwaldi, K. Xie, A. Ablat, S. Dulat, T.-J. Hou, and C. P. Yuan (CTEQ-TEA Collaboration), Precision studies of the post-CT18 LHC Drell-Yan data in the CTEQ-TEA global analysis, Phys. Rev. D **108**, 034030 (2023).
[12] S. Moch, B. Ruijl, T. Ueda, J. A. M. Vermaseren, and A. Vogt, Four-loop non-singlet splitting functions in the planar limit and beyond, J. High Energy Phys. 10 (2017) 041.
[13] G. Falcioni, F. Herzog, S. Moch, and A. Vogt, Four-loop splitting functions in QCD—The gluon-to-quark case, Phys. Lett. B **846**, 138215 (2023).
[14] G. Falcioni, F. Herzog, S. Moch, and A. Vogt, Four-loop splitting functions in QCD: The quark-quark case, Phys. Lett. B **842**, 137944 (2023).
[15] S. Moch, B. Ruijl, T. Ueda, J. Vermaseren, and A. Vogt, Additional moments and x-space approximations of four-loop splitting functions in QCD, Phys. Lett. B **849**, 138468 (2024).
[16] S. Moch, B. Ruijl, T. Ueda, J. A. M. Vermaseren, and A. Vogt, Low moments of the four-loop splitting functions in QCD, Phys. Lett. B **825**, 136853 (2022).
[17] G. Falcioni, F. Herzog, S. Moch, J. Vermaseren, and A. Vogt, The double fermionic contribution to the four-loop quark-to-gluon splitting function, Phys. Lett. B **848**, 138351 (2024).
[18] T. Gehrmann, A. von Manteuffel, V. Sotnikov, and T.-Z. Yang, Complete N_f^2 contributions to four-loop pure-singlet splitting functions, J. High Energy Phys. 01 (2024) 029.
[19] T. Gehrmann, A. von Manteuffel, V. Sotnikov, and T.-Z. Yang, The NfCF3 contribution to the non-singlet splitting function at four-loop order, Phys. Lett. B **849**, 138427 (2024).
[20] X. Ji, Parton physics on a euclidean lattice, Phys. Rev. Lett. **110**, 262002 (2013).
[21] X. Ji, Parton physics from large-momentum effective field theory, Sci. China Phys. Mech. Astron. **57**, 1407 (2014).
[22] M. Constantinou *et al.*, Lattice QCD calculations of parton physics, arXiv:2202.07193.
[23] A. V. Radyushkin, Quasi-parton distribution functions, momentum distributions, and pseudo-parton distribution functions, Phys. Rev. D **96**, 034025 (2017).
[24] A. J. Chambers, R. Horsley, Y. Nakamura, H. Perlt, P. E. L. Rakow, G. Schierholz, A. Schiller, K. Somfleth, R. D. Young, and J. M. Zanotti, Nucleon structure functions from operator product expansion on the lattice, Phys. Rev. Lett. **118**, 242001 (2017).
[25] Y.-Q. Ma and J.-W. Qiu, Exploring partonic structure of hadrons using *abinitio* lattice QCD calculations, Phys. Rev. Lett. **120**, 022003 (2018).
[26] Y.-Q. Ma and J.-W. Qiu, Extracting parton distribution functions from lattice QCD calculations, Phys. Rev. D **98**, 074021 (2018).
[27] L.-B. Chen, W. Wang, and R. Zhu, Next-to-next-to-leading order calculation of quasiparton distribution functions, Phys. Rev. Lett. **126**, 072002 (2021).
[28] Z.-Y. Li, Y.-Q. Ma, and J.-W. Qiu, Extraction of next-to-next-to-leading-order parton distribution functions from lattice QCD calculations, Phys. Rev. Lett. **126**, 072001 (2021).
[29] X. Gao, A. D. Hanlon, S. Mukherjee, P. Petreczky, P. Scior, S. Syritsyn, and Y. Zhao, Lattice QCD determination of the Bjorken-x dependence of parton distribution functions at next-to-next-to-leading order, Phys. Rev. Lett. **128**, 142003 (2022).
[30] M. Bhat, W. Chomicki, K. Cichy, M. Constantinou, J. R. Green, and A. Scapellato, Continuum limit of parton distribution functions from the pseudodistribution approach on the lattice, Phys. Rev. D **106**, 054504 (2022).
[31] X. Gao, A. D. Hanlon, N. Karthik, S. Mukherjee, P. Petreczky, P. Scior, S. Shi, S. Syritsyn, Y. Zhao, and K. Zhou, Continuum-extrapolated NNLO valence PDF of the pion at the physical point, Phys. Rev. D **106**, 114510 (2022).
[32] X. Gao, A. D. Hanlon, J. Holligan, N. Karthik, S. Mukherjee, P. Petreczky, S. Syritsyn, and Y. Zhao, Unpolarized proton PDF at NNLO from lattice QCD with physical quark masses, Phys. Rev. D **107**, 074509 (2023).
[33] J. Holligan and H.-W. Lin, Pion valence quark distribution at physical pion mass of $N_f = 2 + 1 + 1$ lattice QCD, J. Phys. G **51**, 065101 (2024).

[34] S. Moch, J. A. M. Vermaseren, and A. Vogt, The three loop splitting functions in QCD: The nonsinglet case, Nucl. Phys. **B688**, 101 (2004).
[35] X. Ji, J.-H. Zhang, and Y. Zhao, Renormalization in large momentum effective theory of parton physics, Phys. Rev. Lett. **120**, 112001 (2018).
[36] T. Ishikawa, Y.-Q. Ma, J.-W. Qiu, and S. Yoshida, Renormalizability of quasiparton distribution functions, Phys. Rev. D **96**, 094019 (2017).
[37] J. Green, K. Jansen, and F. Steffens, Nonperturbative renormalization of nonlocal quark bilinears for parton quasidistribution functions on the lattice using an auxiliary field, Phys. Rev. Lett. **121**, 022004 (2018).
[38] T. Izubuchi, X. Ji, L. Jin, I. W. Stewart, and Y. Zhao, Factorization theorem relating euclidean and light-cone parton distributions, Phys. Rev. D **98**, 056004 (2018).
[39] G. Curci, W. Furmanski, and R. Petronzio, Evolution of parton densities beyond leading order: The nonsinglet case, Nucl. Phys. **B175**, 27 (1980).
[40] K. G. Chetyrkin and F. V. Tkachov, Integration by parts: The algorithm to calculate β-functions in 4 loops, Nucl. Phys. **B192**, 159 (1981).
[41] S. Laporta, High-precision calculation of multiloop Feynman integrals by difference equations, Int. J. Mod. Phys. A **15**, 5087 (2000).
[42] X. Guan, X. Liu, Y.-Q. Ma, and W.-H. Wu, BLADE: A package for block-triangular form improved Feynman integrals decomposition, Comput. Phys. Commun. **310**, 109538 (2025).
[43] X. Guan, X. Liu, and Y.-Q. Ma, Complete reduction of integrals in two-loop five-light-parton scattering amplitudes, Chin. Phys. C **44**, 093106 (2020).
[44] R. N. Lee, LITERED1.4: A powerful tool for reduction of multiloop integrals, J. Phys. Conf. Ser. **523**, 012059 (2014).
[45] T. Peraro, FINITEFLOW: Multivariate functional reconstruction using finite fields and dataflow graphs, J. High Energy Phys. 07 (2019) 031.
[46] A. V. Kotikov, Differential equations method: New technique for massive Feynman diagrams calculation, Phys. Lett. B **254**, 158 (1991).
[47] X. Liu, Y.-Q. Ma, and C.-Y. Wang, A systematic and efficient method to compute multi-loop master integrals, Phys. Lett. B **779**, 353 (2018).
[48] X. Liu, Y.-Q. Ma, W. Tao, and P. Zhang, Calculation of Feynman loop integration and phase-space integration via auxiliary mass flow, Chin. Phys. C **45**, 013115 (2021).
[49] X. Liu and Y.-Q. Ma, Multiloop corrections for collider processes using auxiliary mass flow, Phys. Rev. D **105**, L051503 (2022).
[50] Z.-F. Liu and Y.-Q. Ma, Automatic computation of Feynman integrals containing linear propagators via auxiliary mass flow, Phys. Rev. D **105**, 074003 (2022).
[51] Z.-F. Liu and Y.-Q. Ma, Determining Feynman integrals with only input from linear algebra, Phys. Rev. Lett. **129**, 222001 (2022).
[52] X. Liu and Y.-Q. Ma, AMFlow: A Mathematica package for Feynman integrals computation via auxiliary mass flow, Comput. Phys. Commun. **283**, 108565 (2023).
[53] V. M. Braun, A. Vladimirov, and J.-H. Zhang, Power corrections and renormalons in parton quasidistributions, Phys. Rev. D **99**, 014013 (2019).
[54] See Supplemental Material at http://link.aps.org/supplemental/10.1103/53ys-3n19 for the matching coefficients at N3LO, with analytical results up to $O(\omega^5)$ and numerical results up to $O(\omega^{100})$.
[55] P. A. Baikov, K. G. Chetyrkin, and J. H. Kühn, Five-loop running of the QCD coupling constant, Phys. Rev. Lett. **118**, 082002 (2017).
[56] R. V. Harlander, S. Y. Klein, and M. Lipp, FEYNGAME, Comput. Phys. Commun. **256**, 107465 (2020).